Ho, C., Lindstrom, T. R., Baldassare, J. J., & Breen, J. J. (1973) *Ann. N.Y. Acad. Sci. 222*, 21–39.
Hvidt, A., & Nielsen, S. O. (1966) *Adv. Protein Chem. 21*, 287–386.
Jue, T., La Mar, G. N., Han, K., & Yamamoto, Y. (1984) *Biophys. J. 46*, 117–120.
Karplus, M., & McCammon, J. A. (1981) *CRC Crit. Rev. Biochem. 9*, 293–349.
Kilmartin, J. V. (1976) *Br. Med. Bull. 32*, 209–212.
Kilmartin, J. V., & Hewitt, J. A. (1971) *Cold Spring Harbor Symp. Quant. Biol. 36*, 311–314.
Kilmartin, J. V., Hewitt, J. A., & Wooton, J. F. (1975) *J. Mol. Biol. 93*, 203–218.
La Mar, G. N., Budd, D. L., & Goff, H. (1977) *Biochem. Biophys. Res. Commun. 77*, 104–110.
La Mar, G. N., Nagai, K., Jue, T., Budd, D. L., Gersonde, K., Sick, H., Kagimoto, T., Hayashi, A., & Tanaka, F. (1980) *Biochem. Biophys. Res. Commun. 96*, 1172–1177.
Leim, R. K. H., Calhoun, D. B., Englander, J. J., & Englander, W. W. (1980) *J. Biol. Chem. 255*, 10687–10694.
Malin, E. L., & Englander, S. W. (1980) *J. Biol. Chem. 255*, 10695–10701.
McCammon, J. A., & Karplus, M. (1983) *Acc. Chem. Res. 16*, 187–193.
Miura, S., & Ho, C. (1982) *Biochemistry 23*, 2492–2499.
Nagai, K., La Mar, G. N., Jue, T., & Bunn, H. F. (1982) *Biochemistry 21*, 842–847.
Nute, P. E., Stamatoyannopoulos, G., Hermodson, M. A., & Roth, D. (1974) *J. Clin. Invest. 53*, 320–328.
Ogawa, S., & Shulman, R. G. (1972) in *Structure and Function of Oxid-Reduction Enzymes* (Akeson, A., & Ehrenberg, A., Eds.) pp 129–131, Pergamon Press, New York, NY.
Ogawa, S., Mayer, A., & Shulman, R. G. (1972) *Biochem. Biophys. Res. Commun. 49*, 1485–1491.
Ogawa, S., Patel, D. J., & Simon, B. R. (1974) *Biochemistry 13*, 2001–2006.
Perutz, M. F. (1970) *Nature 28*, 726–729.
Perutz, M. F. (1976) *Br. Med. Bull. 32*, 195–208.
Perutz, M. F., Ladner, J. E., Simon, S. R., & Ho, C. (1974) *Biochemistry 13*, 2163–2173.
Pettigrew, D. W., Romeo, P. H., Tsapis, A., Thillet, J., Smith, M. L., Turner, B. W., & Ackers, G. K. (1982) *Proc. Natl. Acad. Sci. U.S.A. 79*, 1849–1853.
Ray, J., & Englander, S. W. (1986) *Biochemistry 25*, 3000–3007.
Reed, C. S., Hampson, R., Gordon, S., Jones, R. T., Novy, M. J., Brimhall, B., Edwards, M. J., & Koler, R. D. (1968) *Blood 31*, 623–632.
Shaeffer, J. R., McDonald, M. J., Turci, S. M., Dinda, D. M., & Bunn, H. F. (1984) *J. Biol. Chem. 259*, 14544–14547.
Shannan, B. (1983) *J. Mol. Biol. 171*, 31–59.
Shih, D. T.-B., Jones, R. T., Imai, K., & Tyuma, I. (1985) *J. Biol. Chem. 260*, 5919–5924.
Takahashi, S., Liem, A. K.-L. C., & Ho, C. (1980) *Biochemistry 19*, 5196–5202.
Takahashi, S., Liem, A. K.-L. C., & Ho, C. (1982) *Biophys. J. 39*, 33–40.
Woodward, C. K., & Hilton, B. D. (1979) *Annu. Rev. Biochem. 8*, 99–127.
Woodward, C. K., Simon, I., & Tuchsen, E. (1982) *Mol. Cell. Biochem. 48*, 135–160.

A Proton Nuclear Magnetic Resonance Study of the Antihypertensive and Antiviral Protein BDS-I from the Sea Anemone *Anemonia sulcata*: Sequential and Stereospecific Resonance Assignment and Secondary Structure†

Paul C. Driscoll,‡ G. Marius Clore,*,‡ Laszlo Beress,§ and Angela M. Gronenborn*,‡

Laboratory of Chemical Physics, National Institute of Diabetes and Digestive and Kidney Diseases, National Institutes of Health, Bethesda, Maryland 20892, and Abteilung Toxikologie, Klinikum der Christian-Albrechts-Universität, Hospitalstrasse 4-6, D2300 Kiel, West Germany

Received June 23, 1988; Revised Manuscript Received September 22, 1988

ABSTRACT: The sequential resonance assignment of the ^{1}H NMR spectrum of the antihypertensive and antiviral protein BDS-I from the sea anemone *Anemonia sulcata* is presented. This is carried out with two-dimensional NMR techniques to identify through-bond and through-space (<5 Å) connectivities. Added spectral complexity arises from the fact that the sample is an approximately 1:1 mixture of two BDS-I isoproteins, (Leu-18)-BDS-I and (Phe-18)-BDS-I. Complete assignments, however, are obtained, largely due to the increased resolution and sensitivity afforded at 600 MHz. In addition, the stereospecific assignment of a large number of β-methylene protons is achieved from an analysis of the pattern of $^3J_{\alpha\beta}$ coupling constants and the relative magnitudes of intraresidue NOEs involving the NH, C$^\alpha$H, and C$^\beta$H protons. Regular secondary structure elements are deduced from a qualitative interpretation of the nuclear Overhauser enhancement, $^3J_{HN\alpha}$ coupling constant, and amide NH exchange data. A triple-stranded antiparallel β-sheet is found to be related to that found in partially homologous sea anemone polypeptide toxins.

Sea anemones contain a number of small pharmacologically active polypeptides of molecular weight around 5000. Some of these, such as ATX-I and ATX-II from *Anemonia sulcata*, AP-A from *Anthopleura xanthogrammica*, and RP-II from *Radianthus paumotensis*, are cardiotoxic and neurotoxic. They act by binding specifically to the Na^+ channel, thereby delaying its inactivation during signal transduction. Recently, a small polypeptide known as BDS-I has been isolated from

† This work was supported by the Intramural AIDS Targeted Antiviral Program of the Office of the Director, NIH (G.M.C. and A.M.G.).
‡ National Institutes of Health.
§ Klinikum der Christian-Albrechts-Universität.

0006-2960/89/0428-2178$01.50/0

Anemonia sulcata (Beress et al., 1985). Unlike the the other small polypeptides, BDS-I is neither cardiotoxic nor neurotoxic. Rather, it reduces blood pressure (Beress et al., 1985). A dose as low as 10 μg/kg given intravenously to cats reduces their diastolic pressure by ~50%, and amounts up to 30 mg/kg are well tolerated with no apparent side effects. Its mode of action, however, is unknown. More recently, it has been found that BDS-I also displays antiviral activity and is capable of completely inhibiting the cytopathic effects of the mouse hepatitis virus strain MHV-A59 on mouse liver cells (Komoto and Beress, unpublished data). Sequence analysis of BDS-I has shown that it is composed of an approximately 1:1 mixture of two 43-residue polypeptides, one with a leucine residue and the other with a phenylalanine residue at position 18 (Beress et al., 1985; Henschen, Walsch, and Beress, unpublished data). Like all the sea anemone toxins mentioned above, BDS-I has six cysteine residues. The extent of sequence homology with the toxins, however, is considerably less than that between the toxins themselves. Additionally, BDS-I is slightly shorter than the toxins (43 as opposed to 46–49 residues).

A number of two-dimensional nuclear magnetic resonance (NMR)[1] studies on the sea anemone toxins have been carried out aimed at obtaining sequential resonance assignments and delineating the main secondary structure elements (Gooley & Norton, 1986a,b; Gooley et al., 1984; Wemmer et al., 1986; Widmer et al., 1988). From these data it appears that the toxins are composed of a three- or four-stranded antiparallel β-sheet connected by loops and turns.

In this paper we present the complete assignment of the ^1H NMR spectrum of BDS-I using two-dimensional NMR techniques to identify through-bond and through-space connectivities (Wüthrich, 1986; Clore & Gronenborn, 1987), followed by stereospecific assignment of a large number of β-methylene protons using a combination of NOE and $^3J_{\alpha\beta}$ coupling constant data. In addition, elements of regular secondary structure are delineated from a qualitative interpretation of the NOE and NH exchange data. In the following paper (Driscoll et al., 1989) the determination of the three-dimensional structure of BDS-I in solution is presented.

Experimental Procedures

Purification of BDS-I and Sample Preparation. The initial steps of the isolation procedure are similar to those described earlier for the isolation of ATX-I and ATX-II (Beress & Beress, 1971; Beress et al., 1975; Schweitz et al., 1981). A total of 5 kg of wet *Anemonia sulcata* was homogenized and extracted with 5 L of ethanol at pH 4.5. After centrifugation (2000*g* for 10 min) the supernatant was collected, and the pellet was reextracted with 5 L of 50% ethanol and centrifuged again. The two supernatants were combined and concentrated at reduced pressure to 1 L, and proteins were precipitated by the addition of 10 L of acetone. After the precipitation was completed at −20 °C for 12 h, the acetone was discarded, and the precipitate was dissolved in 1 L of distilled water and subsequently dialyzed against 2 × 20 L of distilled water. Proteins that precipitated during dialysis were removed by centrifugation. The supernatant was passed through a SP-Sephadex C-25 column (7 × 50 cm) at pH 3.5 and at a conductivity of 3 mS, and the bound basic proteins were eluted with 1 M ammonium acetate, pH 9. The resulting eluate was dialyzed against 20 L of distilled water and then concentrated at reduced pressure. The concentrated eluate was filtered on a Sephadex G-50 column (7 × 140 cm). BDS-I and the other small toxins (e.g., ATX-II) were eluted together in the third peak. After freeze-drying, about 9 g of a mixture of basic polypeptides was obtained. BDS-I was purified from this mixture by column ion-exchange chromatography using SP-Sephadex C-25 with a gradient of 0.05–0.3 M ammonium acetate, pH 6. After desalting over Sephadex G-25, approximately 50 mg of BDS-I was obtained. Final purification was carried out by HPLC on a Vydac RP C18 reverse-phase column using 10 mM trifluoroacetic acid with an acetonitrile gradient of 10–50%. Sequence analysis of this material (Beress et al., 1975; Henschen, Walsch, and Beress, unpublished data) revealed that it was composed of an approximately 1:1 mixture of two 43-residue polypeptides differing at position 18:(Leu-18)-BDS-I and (Phe-18)-BDS-I.

Samples for NMR spectroscopy contained approximately 5 mM BDS-I in either 90% H_2O/10% D_2O or 99.996% D_2O, pH 3.

NMR Spectroscopy. NMR spectra were recorded on a Bruker AM600 spectrometer equipped with digital phase shifters, a "reverse"-mode ^1H probe, and an ASPECT 3000 computer. All two-dimensional spectra were recorded in the pure phase absorption mode according to the time proportional phase incrementation (TPPI) method (Redfield & Kuntz, 1975; Bodenhausen et al., 1980) as described by Marion and Wüthrich (1983).

NOESY (Jeener et al., 1979; Macura et al., 1981) and HOHAHA (Braunschweiler & Ernst, 1983; Davis & Bax, 1985; Bax & Davis, 1985a) spectra were recorded at 27 and 19 °C in both D_2O and H_2O. For the NOESY experiments mixing times of 50, 120, and 200 ms were employed. At the shorter mixing time zero-quantum coherence effects were suppressed with either a 5% random variation of the mixing time or a systematic procedure similar to that described by Rance et al. (1985) (A. Bax, private communication). For the HOHAHA experiments all RF pulses were generated via the high-power decoupler channel (90° pulse, ~25–27 μs), with a WALTZ-17_y spin lock sequence (Bax, 1988); 1.5-ms "trim" pulses bracketed the WALTZ-17_y sequence. Total mixing times used were of the order of 18, 33, and 55 ms. For measurements in H_2O the water resonance was suppressed by a semiselective "jump and return" sequence ($90°_x$–τ–$90°_{-x}$) (Plateau & Gueron, 1982) in place of the last 90° pulse of the NOESY sequence and, preceded by a 90° "flip-back" pulse and 100-μs delay, after the mixing period in the HOHAHA experiments (Bax et al., 1987). A τ value of 90 μs was used with an 8-kHz sweep width. Additionally, the adverse effects of radiation damping were partially avoided by cycling the phase of the mixing pulse 45° out of register with those of the preparation and detection periods (Bax, Clore, Driscoll and Gronenborn, unpublished data). That is to say that, for the NOESY sequence $90_{\phi1}$–t_1–$90_{\phi2}$–τ_m–$90_{\phi3}$–acquisition the minimum phase cycling is given by $\phi1 = x, -x$; $\phi2 = x + 45°$: $\phi3 = 2(x), 2(y), 2(-x), 2(-y)$; and receiver = $x, -x, y, -y, -x, x, -y, y$ (where $x = 0°$, $y = 90°$, $-x = 180°$, and $-y = 270°$). This ensures that radiation damping starts immediately after the detection pulse and that the water resonance is never fully inverted along the $-z$ axis, thereby reducing the magnitude of the radiation damping. Optimization of the receiver phase was performed to eliminate base-line distortions (Marion & Bax, 1988). Suppression of undesirable t_2 ridges arising from the strong solvent resonance was achieved by zeroing the first

[1] Abbreviations: NMR, nuclear magnetic resonance; NOE, nuclear Overhauser effect; NOESY, two-dimensional NOE spectroscopy; COSY, homonuclear two-dimensional correlated spectroscopy; DQF-COSY, double quantum filtered correlated spectroscopy; E-COSY, exclusive correlated spectroscopy; HOHAHA, two-dimensional homonuclear Hartmann–Hahn spectroscopy; FID, free induction decay.

point of each FID and by linear base-line corrections of both the initial FIDs (which improves the line shape of the residual H_2O signal) and F_2 cross sections prior to Fourier transformation in F_1. Typically 800–1024 increments of 2K data points were collected per experiment yielding, after zero filling, spectra with digital resolution of the order of 6–8 Hz/pt in each dimension. Lorentz-to-Gaussian convolution was applied in F_2 and a $\pi/5$ phase-shifted sine-squared bell window function in F_1.

DQF-COSY spectra (Rance et al., 1983) were also recorded in D_2O and H_2O at 27 °C and in D_2O at 45 °C. Suppression of the solvent resonance was achieved by selective irradiation during the relaxation delay period. A $\pi/8$ phase-shifted sine bell window function was utilized in data processing in both dimensions.

For the accurate measurement of $^3J_{\alpha\beta}$ coupling constants, E-COSY spectra (Griesinger et al., 1982, 1987) were recorded in D_2O at 27 and 40 °C with presaturation of the residual HOD solvent resonance. A 64-step phase-cycling scheme was used for this experiment (Griesinger et al., 1987). A total of 900 increments of 4K data points were acquired, with a sweep width of 6.4 kHz. For analysis, zero filling was employed to increase the digital resolution to 0.78 Hz/pt in F_2 and 3.13 Hz/pt in F_1. A $\pi/8$ phase-shifted sine bell window function was applied in both dimensions.

Results and Discussion

Assignment of the ^1H NMR Spectrum of BDS-I. The complete assignment of the ^1H NMR spectrum of BDS-I was performed with well-established procedures [see Wüthrich (1986) and Clore and Gronenborn (1987) for reviews]. Two-dimensional NMR spectroscopy (Ernst et al., 1987) was used to identify intraresidue through-bond connectivities (COSY, HOHAHA), followed by the identification of sequential interresidue through-space (<5 Å) connectivities (NOESY). These methods have been successfully applied to a number of small proteins of molecular weight < 10 000.

The sample of BDS-I available to us was a mixture of two isoproteins, approximately 50% (Leu-18)-BDS-I and 50% (Phe-18)-BDS-I. Heterogeneity of the sample has proven to be a complicating factor in the ability to assign the spectra of several proteins. In the case of the ATX-I toxin, also isolated from *Anemonia sulcata*, it was necessary to isolate pure forms of the isoproteins in order to assign the NMR spectrum (Widmer et al., 1988). Initial studies with BDS-I, performed at 500 MHz, indicated that the general features of the spectra of the two forms were very similar. However, slight differences in the chemical shifts of many signals gave rise to a "broad" appearance of many resonances in the 1D NMR spectrum and a "distorted" line shape to the cross-peaks in 2D NMR spectra. As with ATX-I, assignment of this 43-residue peptide was therefore made more difficult than might otherwise be expected. The superior resolution and sensitivity available with a 600-MHz spectrometer, however, allowed us to complete the assignment of both forms of the protein without necessitating their separation. Examples of HOHAHA and NOESY spectra are shown in Figures 1–3.

An important stage in the assignment process was the rationalization of partially overlapping cross-peaks in the HOHAHA spectrum, arising from the same protons in each of the two forms of the protein, by careful analysis of the 600-MHz DQF-COSY spectrum. This is illustrated in Figure 4 which shows the region of a DQF-COSY spectrum, recorded at 45 °C, that includes the methyl group cross-peaks of the leucine and isoleucine residues of BDS-I. In contrast to the HOHAHA spectrum, the characteristic cross-peak patterns of these spin systems are easily discerned in this experiment, allowing the unambiguous identification of three pairs of closely spaced leucine $C^\gamma H$–$C^\delta H_3$ cross-peaks, two close together and another pair further apart. The latter pair of peaks is identified in the sequential assignment analysis as arising from Leu-18 in (Leu-18)-BDS-I. The other peaks are found to arise from the remaining leucine residue Leu-15, with one pair from each of the two forms of the protein. In a similar manner the $C^\beta H$–$C^\gamma H_3$ and $C^\gamma H_2$–$C^\delta H_3$ cross-peaks of Ile-17 in the two forms of the protein are seen to exhibit significantly different chemical shifts. This residue had proved difficult to assign in the analysis of the HOHAHA spectrum since the $C^\alpha H$ protons possess virtually degenerate chemical shifts and two strong $C^\alpha H$–$C^\gamma H_3$ relayed connectivities gave the false impression of a pair of leucine $C^\alpha H$–$C^\delta H_3$ peaks. Also visible in Figure 4 is the slight nondegeneracy in one of the $C^\gamma H_2$–$C^\delta H_3$ cross-peaks of Ile-38. This is not readily detectable in the HOHAHA spectrum recorded at the lower temperature of 27 °C and does not give rise to any difficulty in the assignment of the two proteins.

A complete list of the assignments, including those of spin systems which are distinguishable (at 27 °C) in the mixture of the two peptides, is given in Table I. A summary of the short-range NOEs involving the NH, $C^\alpha H$, and $C^\beta H$ protons, as well as $C^\delta H$ protons of proline, is shown in Figure 5. Note that, qualitatively, no differences were found in the pattern or magnitude of these NOEs for the two forms of the protein.

Points of interest in the assignment of the peptide are the large proportion of extended stretches of $d_{\alpha N}(i,i+1)$ connectivities with accompanying large values (≥8 Hz) of the $^3J_{HN\alpha}$ coupling constants indicative of extended β-strands in the protein structure, and the absence of any helical content, demonstrated by the lack of significant stretches of $d_{NN}(i,i+1)$ NOEs. The Trp-35–Pro-36 and Try-41–Pro-42 connections were both identified as possessing cis peptide bonds on the basis of $d_{\alpha P\alpha}(35,36)$ and $\Delta_{N\alpha}(35,36)$NOEs, and a pair of $d_{\beta P\alpha}(41,42)$NOEs, respectively, coupled with the absence in each case of a $d_{\alpha P\delta}(i,i+1)$ NOE normally associated with a trans peptide bond.

Through observations of the temperature dependence of the 1D NMR spectrum and a comparison of 100-ms NOESY and 50-ms ROESY (Bothner-By et al., 1984; Bax & Davis, 1985b) spectra recorded at 27 °C (not shown), the side chain of Tyr-28 was identified as slowly flipping on the NMR time scale, with distinct chemical shifts for each of the two $C^\delta H$ and $C^\epsilon H$ protons. A possible explanation for the slow flipping of the tyrosine is discussed in the following paper (Driscoll et al., 1989) in the light of the three-dimensional structure of BDS-I.

All residues, with the exception of the N-terminal NH_3^+ group of Ala-1, were completely assigned in both forms of the protein to an accuracy of ±0.01 ppm at 27 °C. Spin systems which exhibit chemical shift differences for the two forms greater than 0.01 ppm fall into two distinct stretches of the protein, namely, Leu-15 to Thr-21 and Tyr-33 to Asn-37 (Table I). While smaller differences could be detected for several other residues, particularly via the cross-peak fine structure of the E-COSY and DQF-COSY spectra recorded at more elevated temperatures, for example Cys-4, it was not possible to attribute them unambiguously to one or the other form of the protein. No evidence was found for multiple conformations of the protein, as has been suggested for the related toxin polypeptides (Wemmer et al., 1986).

Table I includes the stereospecific assignments of the β-methylene protons for several residues. These, together with

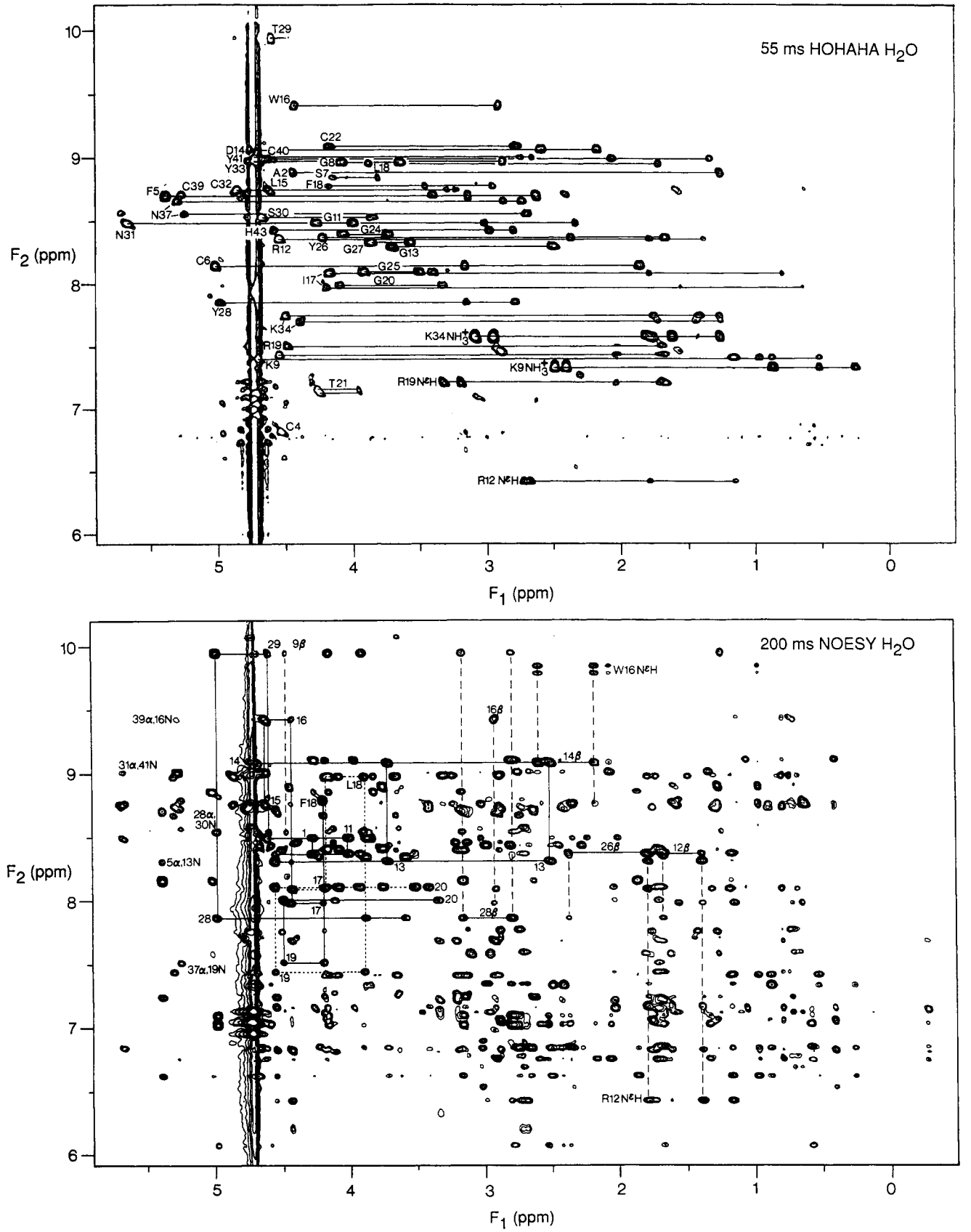

FIGURE 1: NH/aromatic (F_2 axis)–aliphatic (F_1 axis) region of the 55-ms HOHAHA and 200-ms NOESY spectra of BDS-I in H_2O at 27 °C. The cross-peaks in the HOHAHA spectrum arise from direct and relayed connectivities and are indicated by continuous lines with the labels at the positions of the direct NH–$C^{\alpha}H$ connectivity. The doubling of resonances due to the heterogeneity of the primary structure is clearly evident for Ile-17, Phe- and Leu-18, Arg-19, Thr-21, Lys-34, and Asn-37. The cross-peaks in the NOESY spectrum arise from through-space connectivities, examples of which are illustrated. Selected stretches of $C^{\alpha}H(i)$–$NH(i + 1)$ and $C^{\beta}H(i)$–$NH(i + 1)$ NOEs are indicated by continuous (—) and dashed (– –) lines, respectively, with the labels at the position of the intraresidue $C^{\alpha}H(i)$–$NH(i)$ and $C^{\beta}H(i)$–$NH(i)$ cross-peaks. In the case of the stretch of $C^{\alpha}H(i)$–$NH(i + 1)$ NOEs from Ile-17 to Gly-20, however, those arising from (Leu-18)-BDS-I and (Phe-18)-BDS-I are indicated by dotted (···) and continuous (—) lines, respectively. In addition a few long range ($|i - j| > 5$) $C^{\alpha}H(i)$–$NH(j)$ NOEs are indicated. Note that the two cross-peaks for the $C^{\alpha}H(37)$–NH(19) long range NOE arise from the two isoforms of the protein.

Table I: Proton Resonance Assignments of BDS-I at pH 3.0 and 27 °C

residue	chemical shift (ppm)[a]			
	NH	$C^{\alpha}H$	$C^{\beta}H$[b]	other
A1[c]	*d*	3.75	0.97	
A2	8.87	4.45	1.27	
	8.89[e]	4.45	1.27	
P3		4.44	1.62, 1.73	$C^{\gamma}H$ 1.86, 1.98; $C^{\delta}H$ 3.59, 3.61
C4	6.81	4.55	3.19, 2.85*	
	6.81[e]	4.53	3.17, 2.88*	
F5	8.68	5.39	3.14, 2.63*	$C^{\delta}H$ 7.21; $C^{\epsilon}H$ 7.13; $C^{\zeta}H$ 7.13
C6	8.14	5.03	3.17, 1.86*	
S7	8.85	4.16	3.81, 3.81	
G8	8.97	3.65, 3.92		
K9	7.41	4.72	0.96, 1.18*	$C^{\gamma}H$ 0.23, 0.52; $C^{\delta}H$ 0.87, 0.87; $C^{\epsilon}H$ 2.49, 2.40; $N^{\zeta}H_3^+$ 7.32
P10		4.61	2.00, 2.22*	$C^{\gamma}H$ 2.05, 2.14; $C^{\delta}H$ 3.61, 3.78
G11	8.48	4.00, 4.27		
R12	8.36	4.54	1.78, 1.39	$C^{\gamma}H$ 1.16, 1.16; $C^{\delta}H$ 2.68, 2.73; $N^{\epsilon}H$ 6.41
G13	8.29	2.50, 3.71		
D14	9.07	4.74	2.17, 2.59*	
L15	8.76	4.64	1.60, 0.63*	$C^{\gamma}H$ 1.13; $C^{\delta}H_3$ 0.70, 0.74
W16	9.41	4.42	2.91, 2.91	$C^{\epsilon 3}H$ 7.68; $C^{\zeta 3}H$ 7.15; $C^{\eta}H$ 6.80; $C^{\zeta 2}H$ 6.82; $C^{\delta 1}H$ 6.75; $N^{\epsilon 1}H^{e}$ 9.83, 9.78
I17	8.08	4.38	1.79	$C^{\gamma}H_3$ 0.80; $C^{\gamma}H_2$ 1.30, 1.18; $C^{\delta}H_3$ 0.67
L18	8.96	3.90	1.73, 1.73	$C^{\gamma}H$ 1.50; $C^{\delta}H_3$ 0.83, 0.74
R19	7.43	4.52	2.02, 1.64	$C^{\gamma}H$ 1.68, 1.68; $C^{\delta}H$ 3.19, 3.33; $N^{\epsilon}H$ 7.20
G20	8.09	3.36, 4.12		
T21	7.15	4.27	3.96	$C^{\gamma}H_3$ 1.05
C22	9.09	4.19	2.78, 2.75	
P23		4.16	1.68, 1.72	$C^{\gamma}H$ −0.29, 0.58; $C^{\delta}H$ 2.41, 2.52
G24	8.40	3.74, 4.08		
G25	8.09	3.50, 3.92		
Y26	8.37	4.22	2.36, 1.65*	$C^{\delta}H$ 6.85; $C^{\epsilon}H$ 6.75
G27	8.33	3.57, 3.87		
Y28	7.85	4.99	3.16, 2.79*	$C^{\delta}H$ 7.11, 7.03; $C^{\epsilon}H$ 6.07, 7.05
T29	9.93	4.60	4.47	$C^{\gamma}H_3$ 1.24
S30	8.53	4.67	3.88, 3.82*	
N31	8.48	5.67	3.02, 2.32*	NH_2 6.53, 6.83
	8.48[e]	5.69	3.00, 2.32*	NH_2 6.53, 6.83
C32	8.74	4.84	3.23, 3.30*	
Y33	8.97	4.72	2.89, 2.89	$C^{\delta}H$ 7.07; $C^{\epsilon}H$ 6.82
	8.97[e]	4.76	2.89, 2.89	$C^{\delta}H$ 7.04; $C^{\epsilon}H$ 6.80
K34	7.74	4.58	1.41, 1.73	$C^{\gamma}H$ 1.27, 1.80; $C^{\delta}H$ 1.62, 1.82; $C^{\epsilon}H$ 2.85, 3.10; $N^{\zeta}H_3^+$ 7.57
W35	8.45	4.21	3.14, 3.18*	$C^{\epsilon 3}H$ 7.37; $C^{\zeta 3}H$ 6.92; $C^{\eta}H$ 7.07; $C^{\zeta 2}H$ 7.27; $C^{\delta 1}H$ 7.24; $N^{\epsilon 1}H$ 10.07
P36		3.68	0.28, 1.85	$C^{\gamma}H$ 1.35, 1.43; $C^{\delta}H$ 3.00, 3.18
N37	8.66	5.30	2.90, 2.74*	NH_2 7.77, 6.78
I38	8.72	4.76	1.74	$C^{\gamma}H_3$ 0.77; $C^{\gamma}H_2$ 1.27, 0.87; $C^{\delta}H_3$ 0.38
C39	8.71	5.26	2.38, 3.42*	
	8.71[e]	5.27	2.41, 3.41*	
C40	8.99	4.63	1.33, 2.07*	
Y41	9.00	4.67	2.65, 2.75*	$C^{\delta}H$ 6.85; $C^{\epsilon}H$ 6.63
P42		4.68	2.45, 2.27*	$C^{\gamma}H$ 2.02, 1.91; $C^{\delta}H$ 3.91, 4.17
H43	8.42	4.61	3.01, 2.83*	$C^{\delta 2}H$ 7.34; $C^{\epsilon 1}H$ 8.62
L15[f]	8.73	4.62	1.57, 0.61*	$C^{\gamma}H$ 1.09; $C^{\delta}H_3$ 0.66, 0.70
I17[f]	7.87	4.38	1.58	$C^{\gamma}H_3$ 0.66; $C^{\gamma}H_2$ 1.38, 1.17; $C^{\delta}H_3$ 0.71
F18[f]	8.78	4.20	2.95, 3.48	$C^{\delta}H$ 7.10, $C^{\epsilon}H$ 7.12; $C^{\zeta}H$ 7.12
R19[f]	7.50	4.52	2.02, 1.64	$C^{\gamma}H$ 1.68, 1.68; $C^{\delta}H$ 3.19, 3.33; $N^{\epsilon}H$ 7.20
G20[f]	7.99	3.27, 4.03		
T21[f]	7.13	4.25	3.95	$C^{\gamma}H_3$ 1.04
Y33[f]	8.97	4.76	2.89, 2.89	$C^{\delta}H$ 7.04; $C^{\epsilon}H$ 6.80
K34[f]	7.69	4.44	1.44, 1.73	$C^{\gamma}H$ 1.27, 1.80; $C^{\delta}H$ 1.62, 1.82; $C^{\epsilon}H$ 2.85, 3.10; NH_3^+ 7.57
W35[f]	8.39	4.14	3.13, 3.20*	$C^{\epsilon 3}H$ 7.39; $C^{\zeta 3}H$ 6.96; $C^{\eta}H$ 7.04; $C^{\zeta 2}H$ 7.24; $C^{\delta 1}H$ 7.24; $N^{\epsilon 1}H$ 10.07
P36[f]	*d*	3.66	0.21, 1.67	$C^{\gamma}H$ 1.18, 1.34; $C^{\delta}H$ 3.00, 3.15
N37[f]	8.56	5.24	2.74, 2.70*	NH_2 7.59, 6.69

[a] Chemcial shifts are expressed relative to 4,4-dimethyl-4-silapentane-1-sulfonate and were measured with respect to 1,4-dioxane at 3.74 ppm as the internal reference. [b] An asterisk indicates that the first chemical shift value corresponds to the $C^{\beta 3}H$ proton and the second value to the $C^{\beta 2}H$ proton (IUPAC notation). [c] Chemical shifts for (Leu-18)-BDS-I, unless otherwise indicated. [d] Resonance not detected. [e] Two spin systems were identified for this residue but could not be unambiguously assigned to (Leu-18)-BDS I or (Phe-18)-BDS-I. [f] Chemical shifts for (Phe-18)-BDS-I where these are distinguishable from those of (Leu-18)-BDS-I.

the χ_1 side-chain torsion angle ranges shown in Figure 5, were derived on the basis of an analysis of the pattern of $^3J_{\alpha\beta}$ coupling constants and the relative magnitudes of intraresidue $C^{\alpha}H$–$C^{\beta}H$ and NH–$C^{\beta}H$ NOEs (Wagner et al., 1987). NOEs were measured from the 50-ms NOESY spectra and $^3J_{\alpha\beta}$ coupling constants from E-COSY spectra.

Qualitative estimates of the relative sizes of the $^3J_{\alpha\beta}$ coupling constants could also be obtained from WALTZ-17 HOHAHA spectra. For example, Figure 6 shows a comparison of an E-COSY spectrum recorded at 40 °C with the 55-ms HOHAHA spectrum recorded at 27 °C in D_2O. There is a qualitative correlation between the active and passive coupling constants for three-spin systems and the $C^{\alpha}H$–$C^{\beta}H$ cross-peak shapes in the HOHAHA spectrum. Theoretical analysis indicates that these cross-peak characteristics arise from the superposition of resolved antiphase components, created during

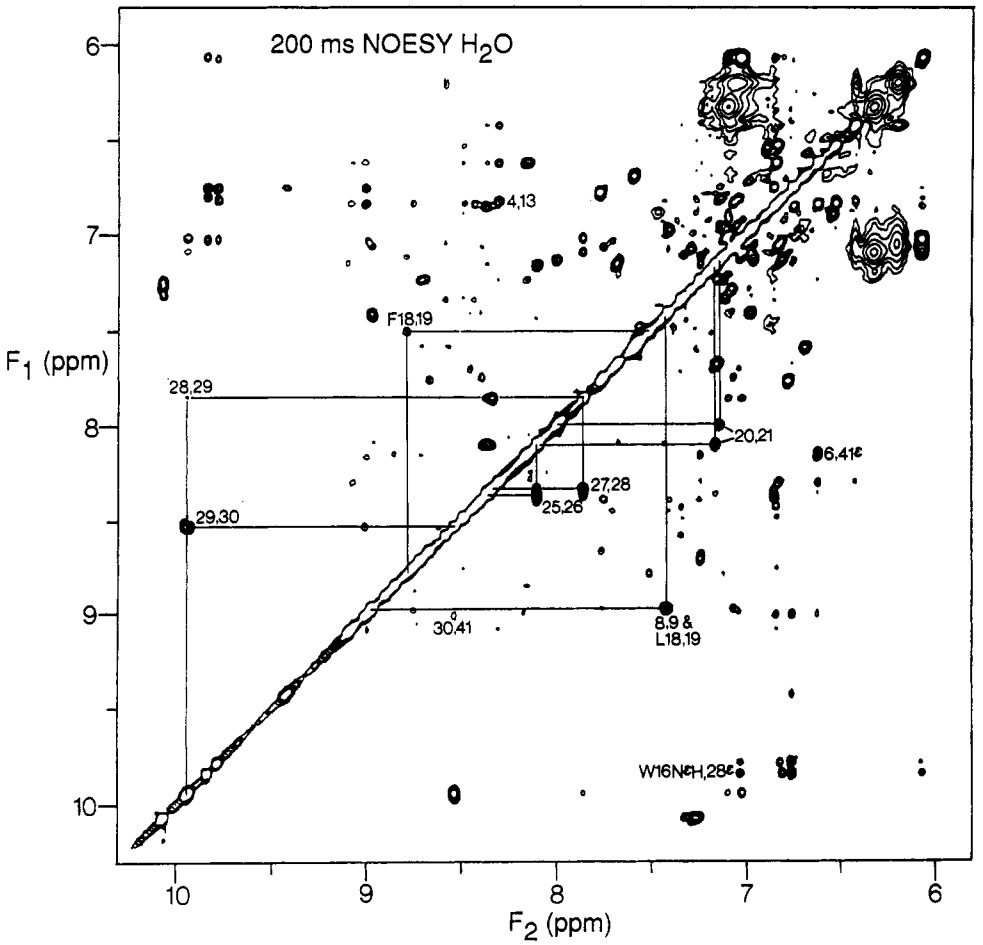

FIGURE 2: NH (F_1 axis)–NH (F_2 axis) region of the 200-ms NOESY spectrum of BDS-I in H_2O at 27 °C. Some sequential ($|i - j| = 1$) and long-range ($|i - j| > 5$) NOE connectivities are indicated. Note the different positions for the sequential NOEs involving Leu-18 and Phe-18 and the doubling up of the NH(20)–NH(21) NOE as a result of the presence of the two isoforms of the protein.

the mixing process, on a pure phase absorption peak (Bax, 1988; Driscoll, Bax, Clore, and Gronenborn, unpublished data). For a $C^{\alpha}H$–$C^{\beta}H$ cross-peak with small (<6.0 Hz) active $^3J_{\alpha\beta^a}$ and large (>10.0 Hz) passive $^3J_{\alpha\beta^b}$ coupling constants (e.g., Asn-37 β_3 in Figure 6), the HOHAHA cross-peak exhibits a double-lobed appearance. For the reverse situation, namely, large active $^3J_{\alpha\beta^a}$ and small passive $^3J_{\alpha\beta^b}$ coupling constants (e.g., Asn-37 β_2 in Figure 6), the HOHAHA cross-peak takes on a four-lobed cross-like shape. For the other common case of both small active $^3J_{\alpha\beta^a}$ and small passive $^3J_{\alpha\beta^b}$ coupling constants (not shown), the HOHAHA cross-peak retains a simple single absorption peak with a relatively small width in the $C^{\alpha}H$ dimension. Figure 6 nicely illustrates the advantages of this observation. First, the qualitative coupling constant information necessary to make stereospecific assignments can potentially be obtained directly by inspecting the HOHAHA spectrum. The HOHAHA spectrum is recorded at a lower temperature than the E-COSY spectrum, for which elevated temperatures are preferred in order to minimize the effects of antiphase cross-peak component overlap (which equally applies to COSY and DQF-COSY experiments). Second, this information can be inferred even in cases where cross-peaks are partially overlapping, as is the case for many residues in the spectrum of BDS-I. Figure 6 includes the $C^{\alpha}H$–$C^{\beta 2}H$ and $C^{\alpha}H$–$C^{\beta 3}H$ cross-peaks of Asn-37 which are well separated for both forms of the protein, the $C^{\alpha}H$–$C^{\beta 3}H$ cross-peaks of both Cys-39 spin systems which partially overlap one another, and the $C^{\alpha}H$–$C^{\beta 2}H$ cross-peaks of both Phe-5 spin systems which appear exactly overlaid. For the Cys-39 cross-peaks it is a relatively easy task to assign a large passive coupling constant despite the overlap. It should be noted, however, that the antiphase components quickly cancel themselves out as the line width increases. Consequently, for larger proteins ($M_r \geq 10000$), the HOHAHA cross-peaks are close to pure phase absorption, and the cross-peak shapes described above are difficult to observe. Thus, the qualitative assessment of coupling constants from HOHAHA spectra will generally only be applicable to proteins with narrow line widths.

Measured values of the $^3J_{HN\alpha}$ coupling constants of >8.0 Hz and <7.0 Hz were interpreted in terms of ϕ torsion angle restraints of $-160° < \phi < -80°$ and $-90° < \phi < -40°$, respectively (Pardi et al., 1984). These torsion angle identifications are included in summary form in Figure 5.

Slowly exchanging NH protons were identified from HOHAHA spectra recorded after dissolution of the peptide, freshly freeze-dried from H_2O, in D_2O. Those NHs still present in the spectrum are indicated in Figure 5.

Identification of Secondary Structure Elements in BDS-I. Regular secondary structure elements are readily identified from a qualitative interpretation of NOE, coupling constant, and NH exchange rate data (Wüthrich et al., 1984; Wagner et al., 1986). In this manner two regular secondary structure elements were identified in BDS-I. These are illustrated schematically in Figure 7.

First, a triple-stranded antiparallel β-sheet, involving two stretches of the protein chain—residues Asp-14 to Ile-17 and Ser-30 to Tyr-41—can be invoked on the basis of the pattern of short-range $d_{\alpha N}(i,i+1)$ and $d_{NN}(i,i+1)$ and long-range $d_{\alpha\alpha}(i,j)$, $d_{\alpha N}(i,j)$, and $d_{NN}(i,j)$ NOEs, the prevalence of large (>9.0 Hz) $^3J_{HN\alpha}$ coupling constants, and long-range side-

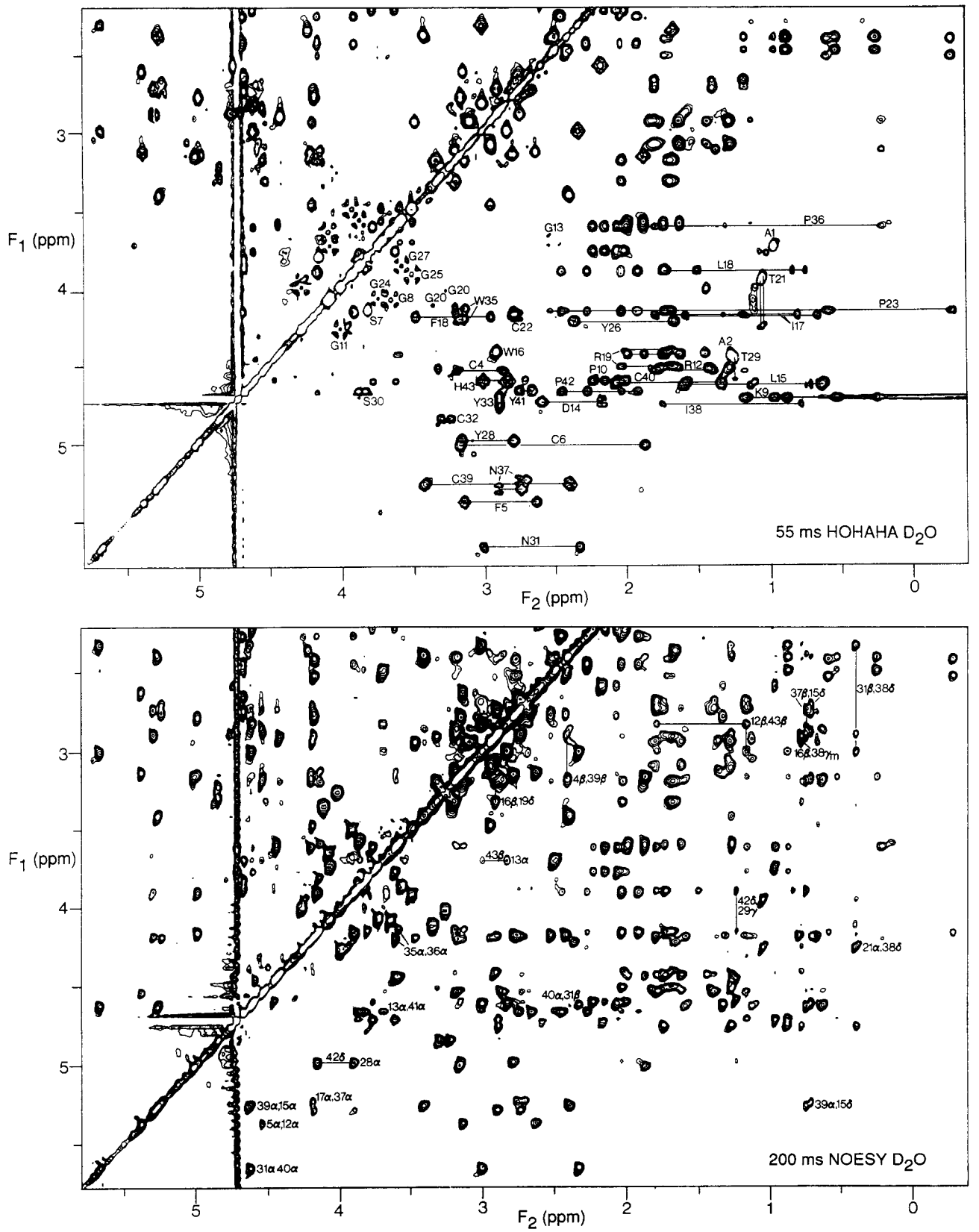

FIGURE 3: Portion of the $C^{\alpha}H$ (F_1 axis)–aliphatic (F_2 axis) region of the 55-ms HOHAHA and 200-ms NOESY spectra of BDS-I in D_2O at 27 °C. Direct and relayed connectivities are present in the HOHAHA spectrum, and some spin networks originating from the $C^{\alpha}H$ protons are indicated by continuous lines. Cross-peaks arising from long range ($|i - j| > 5$) NOEs are labeled in the NOESY spectrum. Note the two NOESY cross-peaks for the $C^{\alpha}H(17)$–$C^{\alpha}H(37)$ connectivity in the two isoforms of the protein.

chain–side-chain NOEs between residues on each of two adjacent strands of the sheet. A reverse turn at positions Trp-35 and Pro-36 is required to enable the completion of the polypeptide chain between strands 2 and 3 (see Figure 7a). As the experimental data indicate a cis peptide bond together with a strong NOE between the $C^{\alpha}H$ protons of these two residues, it is likely that the reverse turn is of type VIa character (Richardson, 1981). The distribution of slowly exchanging backbone amide NH protons can be rationalized on the basis of this secondary structure element as forming interstrand

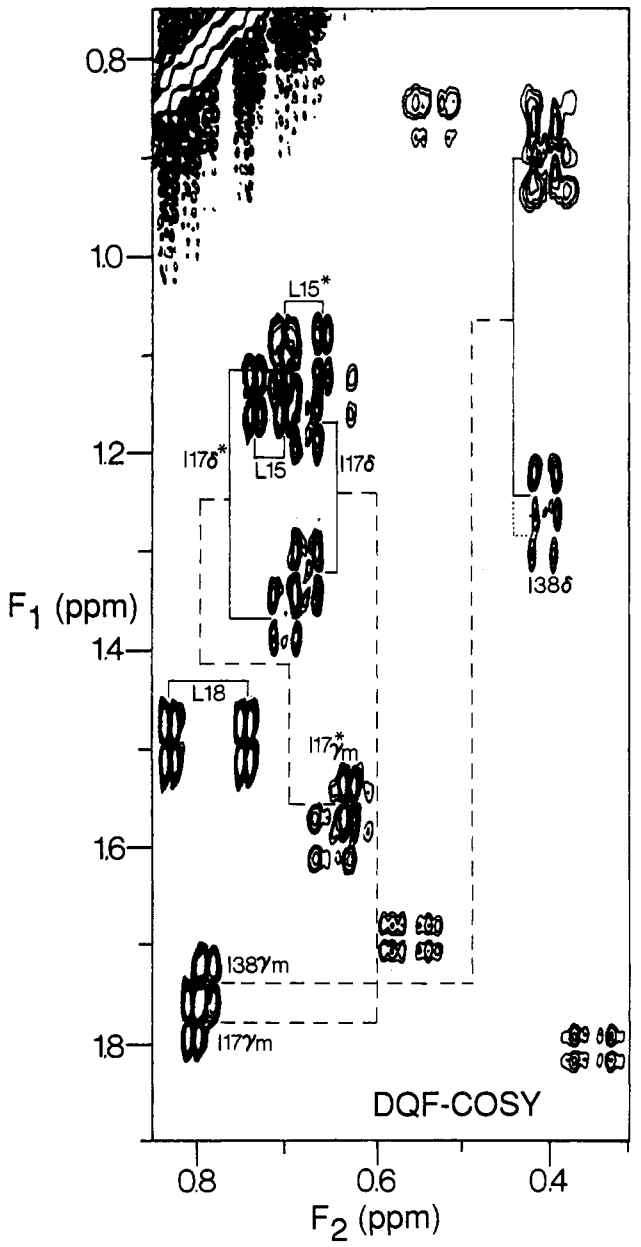

FIGURE 4: Methyl group cross-peak region of the DQF-COSY spectrum of BDS-I recorded at 45 °C, illustrating the doubling of resonances due to heterogeneity of the molecule at position 18. Note the two sets of cross-peaks for Leu-15 and Ile-17. An asterisk indicates that the spin system arises from (Phe-18)-BDS-I. Positive and negative contour levels are not distinguished.

hydrogen bonds as shown in Figure 7a.

A second element of secondary structure has been identified for residues Cys-6, Ser-7, Gly-8, and Lys-9. This tetrapeptide segment takes the form of a reverse turn with residues Cys-6 and Lys-9 forming a miniature antiparallel β-sheet. Hydrogen bonds are readily identified between the amide NH of Cys-6 and the carbonyl oxygen of Lys-9, and vice versa. A strong $d_{NN}(i,i+1)$ NOE between residues Gly-8 and Lys-9 and a strong $d_{\alpha N}(i,i+1)$ NOE between residues Gly-8 and Ser-7 indicate that this structural element has the characteristics of a regular type II turn (see Figure 7b).

As for the rest of the protein, no obvious secondary structure can be unambiguously identified. Residues Ala-1 to Cys-4, including Pro-3, and Pro-10 to Gly-13 are thought to be in extended strands due to the absence of strong $d_{NN}(i,i+1)$-type NOEs. The loop between Ile-17 at one end of strand 1 of the three-stranded β-sheet and Ser-30 at the end of strand 3 at the opposite end of the sheet comprises residues connected by a mixture of both $d_{NN}(i,i+1)$ and $d_{\alpha N}(i,i+1)$ NOEs (see Figure 5). No regular secondary structure elements could be elucidated by simple inspection of this data. The precise structure of the remaining C-terminal Tyr-41 to His-43 segment of the protein is likewise not clear from a qualitative analysis of the data.

At this stage it is possible to compare the secondary structure of BDS-I with that for the related sea anenome toxins ATX-I, AP-A, and RP-II (Widmer et al., 1988; Gooley & Norton, 1986b; Wemmer et al., 1986). In all cases β-sheet structural elements connected by ill-defined loops have been described. Figure 8 illustrates in tabular form the β-sheet structures that have been identified for these proteins from qualitative analysis of NMR data. Most detailed information has been produced for ATX-I (Widmer et al, 1988), which is thought to contain a four-stranded antiparallel β-sheet, within which the relative placement of four cysteine residues is identical with that found in the present study of BDS-I: Cysteines-4, -34, -43, and -44 of ATX-I correspond to cysteines-4, -32, -39, and -40 of BDS-I. Note that for BDS-I Cys-4 is not found in an extended strand as part of the β-sheet; rather, it is connected to the triple-stranded β-sheet by a long-range d_{NN} NOE connectivity to Gly-13, combined with NOE and NH exchange rate evidence for a hydrogen bond between Gly-13 NH and Cys-4 CO. Identical relative placements of cysteine residues are also found in the four-stranded β-sheets of AP-A (Gooley & Norton, 1986b) and RP-II (Wemmer et al., 1986). Figure 8 also illustrates that residues corresponding to Gly-13, Leu-15, Trp-16, and Asn-31 in the β-sheet of BDS-I are strongly conserved in the β-sheets of the toxins ATX-I from *Anemonia sulcata* and AP-A from *Anthopleura xanthogrammica*. The toxin RP-II, which is isolated from the sea anenome *Radianthus paumotensis*, exhibits similar, though less extensive, structural homology. For example, a lysine residue (Lys-32) is found at the position of the conserved asparagine in the other peptides. On the other hand, it is noticeable that BDS-I lacks a positively charged residue at the position in the β-sheet corresponding to Tyr-41—all the other polypeptides have either lysine or arginine at this position—and possesses an aspartic acid residue at position 14, where the toxins mostly have a threonine side chain (ATX-II, with 62% sequence homology with ATX-I, has isoleucine at this position).

Concluding Remarks

In this paper we have presented the sequential assignment of the antihypertensive and antiviral polypeptide BDS-I from the sea anenome *Anemonia sulcata*. This has been achieved, despite the difficulties arising from heterogeneity which leads to a large number of partially overlapping cross-peaks in the 2D NMR spectrum, with a combination of HOHAHA and DQF-COSY spectroscopy together with sequential analysis of NOESY spectra. In addition, stereospecific assignments for a large number of β-methylene protons were made, and a method for qualitatively assessing the magnitude of $^3J_{\alpha\beta}$ coupling constants from the fine structure of HOHAHA cross-peaks has been described. From a qualitative analysis of the NMR results, two regular secondary structure elements have been identified and shown to be related to previously described structural elements in the partially homologous cardiotoxic and neurotoxic peptides ATX-I, ATX-II, AP-A, and RP-II.

It has been noted that the neurotoxic and cardiotoxic effects of the ATX and RP classes of polypeptides are subtly different with regard to their binding to Na^+ channels from different

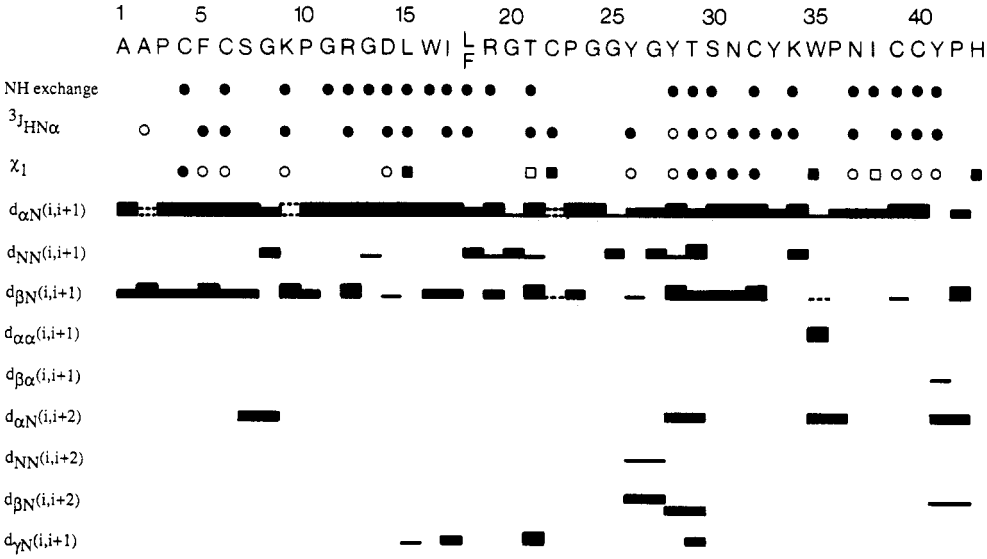

FIGURE 5: Sequence of BDS-I together with a summary of all the short-range NOEs involving the NH, $C^{\alpha}H$, and $C^{\beta}H$ protons, as well as the $C^{\delta}H$ protons of proline residues, the slowly exchanging NH protons, the $^3J_{HN\alpha}$ coupling constants, and the χ_1 side-chain torsion angles. The NOEs are classified as strong, medium, and weak by the thickness of the lines. The $C^{\alpha}H(i)$–$C^{\delta}H(i+1)$ and $C^{\beta}H(i)$–$C^{\delta}H(i+1)$ NOEs involving a proline residue at position $i+1$ are indicated as a dashed box along the same line as the $C^{\alpha}H(i)$–$NH(i+1)$ and $C^{\beta}H(i)$–$NH(i+1)$ NOEs, respectively. NH protons that are still present after 12 h of the protein being dissolved in D_2O are indicated by closed circles. $^3J_{HN\alpha}$ coupling constants >8 Hz are indicated by closed circles (●) and those <7 Hz by open circles (○). The ranges for the χ_1 side-chain torsion angles, derived from the $^3J_{\alpha\beta}$ coupling constants and the pattern of intraresidue NH–$C^{\alpha}H$ and NH–$C^{\beta}H$ NOEs, are as follows: (●) $0° < \chi_1 < 120°$; (■) $120° \chi_1 < 240°$; (○) $-120° < \chi_1 < 0°$; (□) $0° < \chi_1 < 240°$.

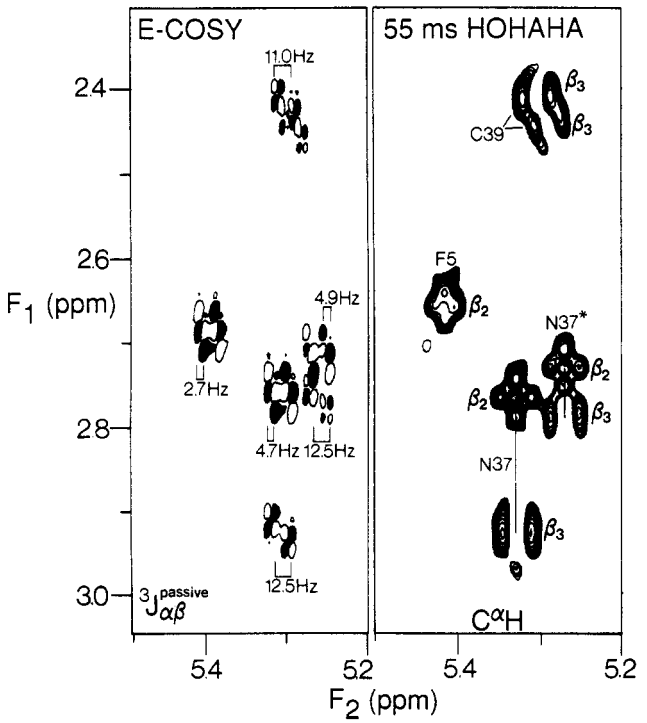

FIGURE 6: Comparison of 55-ms HOHAHA (27 °C) and E-COSY (45 °C) spectra displaying cross-peak shapes for selected AMX spin systems of BDS-I. Note that the relative magnitude of the passive $^3J_{\alpha\beta}$ coupling constants can be directly visualized from the shape of the HOHAHA peaks. An asterisk indicates the Asn-37 cross-peaks from (Phe-18)-BDS-I. Positive and negative components of the E-COSY cross peaks are distinguished by filled and open contour levels. The stereospecific assignment of the $C^{\beta}H$ protons is shown in the HOHAHA spectrum.

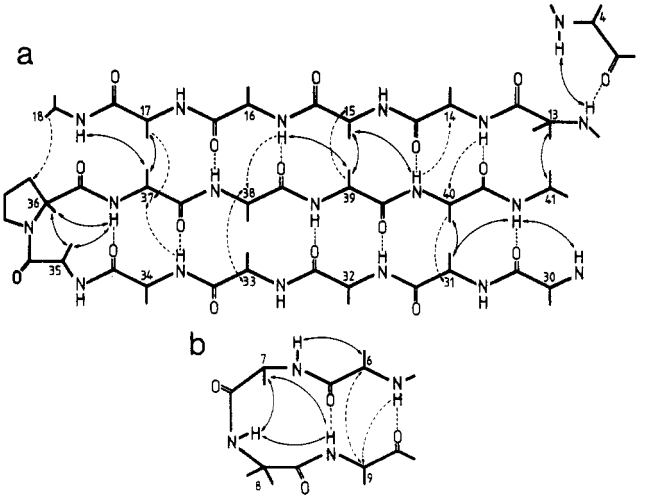

FIGURE 7: Schematic representation of (a) the triple-stranded β-sheet and (b) the type II tight turn in the structure of BDS-I, deduced from the qualitative analysis of NMR data, including the pattern of sequential NOES, long-range backbone to backbone NOEs (↔), backbone to $C^{\beta}H$ NOEs (--►), side-chain to side-chain NOEs (►--►), and the identification of slowly exchanging amide NH protons involved in hydrogen-bond formation (---).

types of cells (Schweitz et al., 1985). The activity of BDS-I as a antihypertensive agent is presumably significantly different, though this could well be mediated through channel binding of some sort (e.g., to the Ca^{2+} channel). The difference in physiological action between BDS-I and the toxins is paralleled by the fact that the sequence homology between the ATX, AP, and RP toxins is much higher than that between any of the toxins and BDS-I. All of these polypeptides, however, have a common structural motif comprising an antiparallel β-sheet, within which a number of structurally important cysteine residues are conserved. This suggests a common evolutionary ancestry. In order to investigate structure–function relationships for this group of molecules, it will be necessary to acquire a more detailed knowledge not only of their three-dimensional structures but also of those regions which are crucial for activity. We have therefore carried out a determination of the three-dimensional solution structure of BDS-I on the basis of the NMR data presented here. This study is described in the following paper (Driscoll et al., 1989).

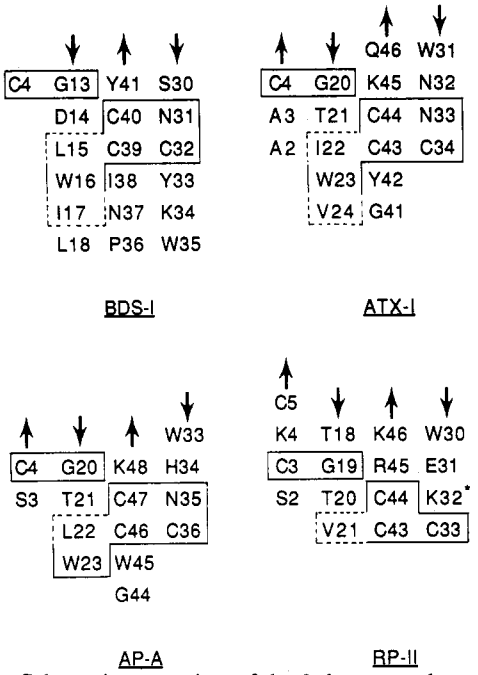

FIGURE 8: Schematic comparison of the β-sheet secondary structure elements obtained from NMR studies of BDS-I from *Anemonia sulcata* with ATX-I (also from *Anemonia sulcata*), AP-A (*Anthopleura xanthogrammica*), and RP-II (*Radianthus paumotensis*) (for references, see text). The conservation of the relative placement of four cysteine and some of the neighboring residues is highlighted in the boxed regions. Full lines indicate strict homology, whereas dashed lines indicate conservative substitutions. An asterisk indicates that Lys-32 of AP-A does not fit in the conserved region. The direction of the β-strands is indicated by arrows. Note that despite these similarities between BDS-I and the toxins a greater degree of homology exists between the toxins themselves (e.g., residues corresponding to Trp-31 and Thr-21 of ATX-I).

ACKNOWLEDGMENTS

We thank Dr. Ad Bax for useful discussions.

Registry No. (Leu-18)-BDS-I, 96510-29-1; (Phe-18)-BDS-I, 118246-78-9.

REFERENCES

Bax, A. (1988) *Methods Enzymol.* (in press).
Bax, A., & Davis, D. G. (1985a) *J. Magn. Reson. 65*, 355–366.
Bax, A., & Davis, D. G. (1985b) *J. Magn. Reson. 63*, 207–213.
Bax, A., Sklenar, V., Clore, G. M., & Gronenborn, A. M. (1987) *J. Am. Chem. Soc. 109*, 6511–6513.
Beress, L., & Beress, R. (1971) *Kiel. Meeresforsch. 27*, 117–127.
Beress, L., Beress, R., & Wunderer, G. (1975) *Toxicon 13*, 359–367.
Beress, L., Doppelfeld, I.-S., Etschenberg, E., Graf, E., Henschen, A., & Zwick, J. (1985) Federal Republic of Germany Patent DE 3324689 A1.
Bodenhausen, G., Vold, R. L., & Vold, R. R. (1980) *J. Magn. Reson. 37*, 93–106.
Bothner-By, A. A., Stephens, R. L., Lee, J. T., Warren, C. D., & Jeanloz, R. W. (1984) *J. Am. Chem. Soc. 106*, 811–812.
Braunschweiler, L. R., & Ernst, R. R. (1983) *J. Magn. Reson. 53*, 521–528.
Clore, G. M., & Gronenborn, A. M. (1987) *Protein Eng. 1*, 275–288.
Davis, D. G., & Bax, A. (1985) *J. Am. Chem. Soc. 107*, 2821–2822.
Driscoll, P. C., Gronenborn, A. M., Beress, L., & Clore, G. M. (1989) *Biochemistry* (following paper in this issue).
Ernst, R. R., Bodenhausen, G., & Wokaun, A. (1986) *Principles of Nuclear Magnetic Resonance in One and Two Dimensions*, Clarendon Press, Oxford.
Gooley, P. R., & Norton, R. S. (1986a) *Biopolymers 25*, 489–506.
Gooley, P. R., & Norton, R. S. (1986b) *Biochemistry 25*, 2349–2356.
Gooley, P. R., Beress, L., & Norton, R. S. (1984) *Biochemistry 23*, 2144–2152.
Griesinger, C., Sørensen, O. W., & Ernst, R. R. (1982) *J. Am. Chem. Soc. 104*, 6800–6802.
Griesinger, C., Sørensen, O. W., & Ernst, R. R. (1987) *J. Magn. Reson. 75*, 474–492.
Jeener, J., Meier, B. H., Bachmann, P., & Ernst, R. R. (1979) *J. Chem. Phys. 71*, 4546–4553.
Macura, C., Huang, Y., Suter, D., & Ernst, R. R. (1981) *J. Magn. Reson. 43*, 259–281.
Marion, D., & Wüthrich, K. (1983) *Biochem. Biophys. Res. Commun. 113*, 967–974.
Marion, D., & Bax, A. (1988) *J. Magn. Reson. 79*, 352–356.
Pardi, A., Billeter, M., & Wüthrich, K. (1984) *J. Mol. Biol. 180*, 741–751.
Plateau, P., & Gueron, M. (1982) *J. Am. Chem. Soc. 104*, 7310–7311.
Rance, M., Sørensen, O. W., Bodenhausen, G., Wagner, G., Ernst, R. R., & Wüthrich, K. (1983) *Biochem. Biophys. Res. Commun. 117*, 479–485.
Rance, M., Bodenhausen, G., Wagner, G., Wüthrich, K., & Ernst, R. R. (1985) *J. Magn. Reson. 62*, 497–510.
Redfield, A. G., & Kuntz, S. D. (1975) *J. Magn. Reson. 19*, 250–254.
Richardson, J. S. (1981) *Adv. Protein Chem. 34*, 167–339.
Schweitz, H., Barhanin, J. P., Frelin, C., Hughes, G., & Lazdunski, M. (1981) *Biochemistry 20*, 5245–5252.
Schweitz, H., Bidard, J.-N., Frelin, C., Pauron, D., Vijverberg, H. P. M., Mahasneh, D. M., & Lazdunski, M. (1985) *Biochemistry 24*, 3554–3561.
Wagner, G., Neuhaus, D., Wörgötter, E., Vasak, M., Kägi, R. J. H., & Wüthrich, K. (1986) *J. Mol. Biol. 187*, 131–135.
Wagner, G., Braun, W., Havel, T. F., Schaumann, T., Go, N., & Wüthrich, K. (1987) *J. Mol. Biol. 196*, 611–639.
Wemmer, D. E., Kumar, N. V., Metrione, R. M., Lazdunski, M., Drobny, G., & Kallenbach, N. R. (1986) *Biochemistry 25*, 6842–6849.
Widmer, A., Wagner, G., Schweitz, N., Lazdunski, M., & Wüthrich, K. (1988) *Eur. J. Biochem. 171*, 177–192.
Wüthrich, K. (1986) *NMR of Proteins and Nucleic Acids*, Wiley, New York.
Wüthrich, K., Billeter, M., & Braun, W. (1984) *J. Mol. Biol. 180*, 715–740.